TECHNICAL NOTE

UV/Visible Spectroscopy

Authors:

Jeffrey L. Taylor, Ph.D.
Chris Lynch
Jillian F. Dlugos

PerkinElmer, Inc.
Shelton, CT

Particle Characterization of UV Blocking Sunscreens and Cosmetics Using UV/Visible Spectroscopy

Introduction

Many cosmetic products now incorporate sunblock components to protect the skin from harmful ultra violet radiation. These products can be identified by the SPF value quoted on the label. A large proportion of these blocking components are nanoparticles that protect the skin, not by absorbing the harmful radiation, but by scattering it away from the skin. The most commonly used are nanoparticles of zinc oxide and titanium dioxide. This paper will discuss a new method for characterization and quantitation of nanoparticles in sunscreens and cosmetics via the use of UV/Visible spectroscopy. The method utilizes a 150 mm integrating sphere equipped with center mount and is able to quantitate and compare the contributions of absorbance, large particle scattering, and nanoparticle scattering.

PerkinElmer®
For the Better

A UV/Visible spectrophotometer fitted with a 150 mm integrating sphere and enter mount is capable of making a number of measurements important to the nanomaterial industry. In this paper we will discuss a methodology to distinguish between nanoparticle scattering, large particle scattering, and sample absorbance. In addition, the nanoparticle characterization method allows for measurements to be made on finished products, such as creams, powders, solids, gels, films, and liquids. The method can also be used for formulation studies, individual product component analysis, and QC analysis of finished products. This method shows potential to be used in a wide variety of marketing segments throughout the nanomaterials industry with feasibility in industrial, food, environmental, and medical/pharmaceutical applications.

The rational behind UV protection inherent in sunscreens and cosmetics that have active ingredients of particulate zinc oxide and titanium dioxide is 1) small particles are very efficient at scattering shorter light wavelengths and 2) perceived reduced long term exposure toxicity of inert particles over benzenoid organic compounds.

Light Scatter

Light scattering is one of the two major physical processes that contribute to the visible appearance of most objects, the other being absorption. Surfaces described as white owe their appearance to multiple scattering of light by internal or surface inhomogeneities in the object, for example by the boundaries of transparent microscopic crystals that make up a stone or by the microscopic fibers in a sheet of paper. More generally, the gloss (or luster or sheen) of the surface is determined by scattering. Highly scattering surfaces are described as being dull or having a matte finish, while the absence of surface scattering leads to a glossy appearance, as with polished metal or stone. Spectral absorption, the selective absorption of certain light wavelengths, determines the color of most objects with some modification by elastic scattering. The apparent blue color of veins in skin is a common example where both spectral absorption and scattering play important and complex roles in the coloration. Light scattering can also create color without absorption, often shades of blue, as with the sky, the human blue iris, certain insect coloration like butterfly wings, and the feathers of some birds are just a few examples.

There are several types of scattering phenomena that we need to be aware of for this study. Mathematical light scattering models, relevant to this study, can be divided into three domains based on the important factor of particle diameter. If the particle is small (< 1/10) compared to the wavelength of incident light, Rayleigh scatter predominates. If the particles are approximately equal in size to the wavelength, Mie scattering predominates. Finally, if the particles are much larger than the wavelength, then geometric Mie scattering is the rule. The key to characterizing particle scattering as a function of UV/Visible spectroscopy is found in the Rayleigh scattering equation depicted in Equation 1. Shown below is the generalized form of the Rayleigh light scattering equation for scattering intensity by a particle. There are numerous factors that contribute to scattering intensity: the distance to the particle, the scattering angle, and the refractive index of the particle.

However, in this investigation, we will be primarily concerned with the two factors of particle size and the wavelength of incident light.

Equation 1:

$$I = I_0 \frac{1+\cos^2\theta}{2R^2}\left(\frac{2\pi}{\lambda}\right)^4\left(\frac{n^2-1}{n^2+2}\right)^2\left(\frac{d}{2}\right)^6$$

Where:
R = distance to the particle
Θ = scattering angle
n = refractive index of particle
d = diameter of particle
λ = wavelength of incident light

Wavelength component

Particle diameter component

Figure 1. The Rayleigh Scatter Equation

Depicted above is the generalized form of the Rayleigh light scattering equation for scattering intensity by a particle. There are numerous factors that contribute to scattering intensity: the distance to the particle, the scattering angle, and the refractive index of the particle. However, we will be primarily concerned with the two factors of particle size and the wavelength of incident light. The incident light wavelength (shaded green in the equation above) relates to the scattering intensity by the inverse 4th power of the wavelength. Nanoparticle scatter is highly dependent on wavelength with shorter wavelengths (ultra violet or blue light) are scattered much more intensely than longer wavelengths (red light). This is why the sky appears blue, because of highly scattered blue light from the gas molecules of the atmosphere. The particle size (diameter) is important also (shaded red in the above equation) and is related to a direct proportion of the 6th power of the diameter. Also large particle (larger than the incident wavelength of light) scatter is not wavelength dependent.

There is a significant difference between Rayleigh and Mie scatter with the distribution envelop of the emitted scatter intensity as a function of angle to the incident light. This is shown in Figure 1a. Note how the Rayleigh scatter has a more even distribution though 360 degrees; whereas, Mie scatter has a forward directed antenna lobe projecting in the general direction of the incident light. Since we will be using an integrating sphere with center mount to collect the data, the angular distribution envelope of the scatter will not be a significant factor.

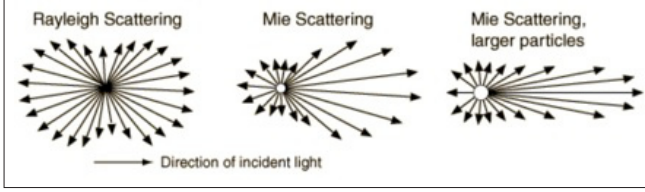

Figure 1a. Types of Scatter

So what are the size ranges that define "large particle" and "nanoparticle" as a function of the Rayleigh scatter equation. In theory, this means that if we are going to use the wavelength range of 1000 nm to 400 nm for particle characterization, the size threshold for "nanoparticles" is less than several hundred nanometers. Large particles would be any particles larger than that range.

The individual parts of the Rayleigh scattering equation can be easily modeled to see how the various components would affect a UV/ Visible spectrum obtained with a spectrophotometer. The spectra displayed in Figure 1b show how nanoparticle based scatter manifests itself in a scatter transmission spectra. Note the extreme wavelength dependency at the shorter wavelengths. Only the inverse fourth power wavelength function of the Rayleigh equation is modeled here. In "real life" the interaction would be much more complex and dependent on multiple conditions. Factors such as particle size, angle of incident light, refractive index, and scattering angle would all combine to modify the curvature of the spectrum. The simple "take home" message here is that nanoparticle scatter curves the baseline component of a UV/ Visible spectrum.

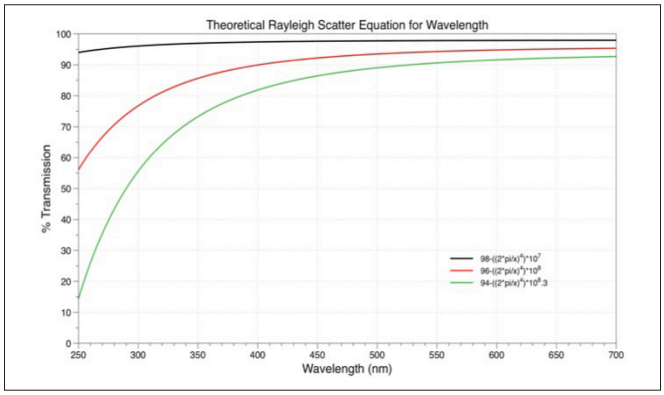

Figure 1b. Theoretical Percent Transmission Spectra Calculated From Rayleigh Equation

Let's see what happens with a "real world" scattering sample and compare it to a simple Rayleigh scattering model. We see in Figure 1c a theoretical spectrum (red) based on the isolated incident light wavelength component of the Rayleigh scatter equation. It has been "normalized" to conform to the long and short wavelength endpoints of a 20% zinc oxide cream sunscreen spectrum (black). As we can see, there is more going on here than simple wavelength dependent nanoparticle scatter. The long wavelength ordinate offset from 100% transmission is due to large particle geometrical Mie type scattering and the ultra-violet region below 400 nanometers has significant absorbance from the sunscreen's cream formulation ingredients. Nanoparticle scatter is just one of several light interactions inherent in modern sunscreens and cosmetics.

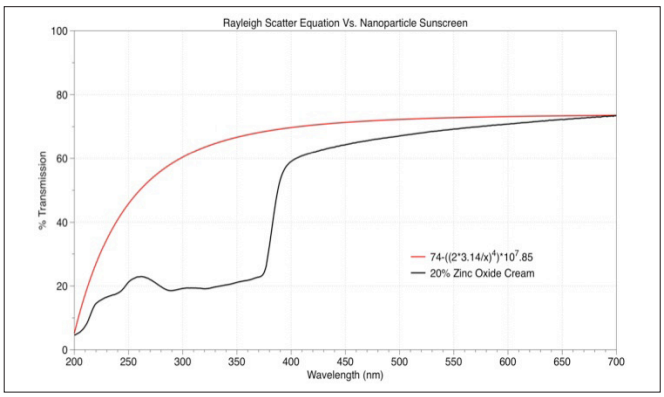

Figure 1c. Theoretical % Transmission Scatter Spectra vs. Typical Sunscreen Spectra

Because of all the complex components of the Rayleigh scattering equation just discussed, it would not do well for mathematical modeling of experimental data. Sunscreens and cosmetics are formulations of many components that give rise to absorbance, large particle scattering, and nanoparticle scattering. We briefly considered trying to model a more manageable cubic polynomial curve fit to the data as seen in Figure 1d.

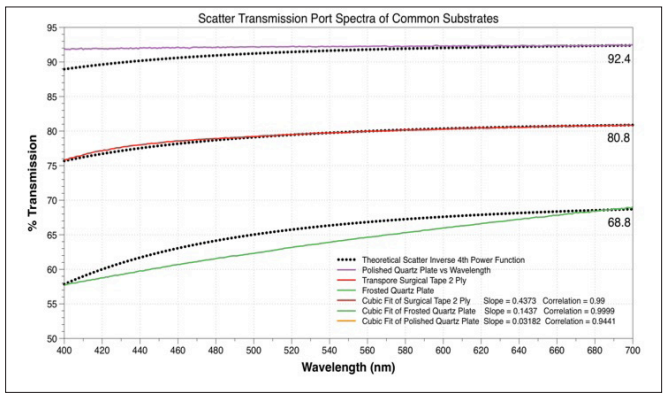

Figure 1d. Comparison of Theoretical Scatter Spectra With Some Typical Scattering Substrates

This graph shows the comparison of both the isolated wavelength part of the Rayleigh scatter equation and a cubic polynomial fit to some examples of scattering media. The Rayleigh scattering equation does not give a consistent fit for a variety of different scattering samples. Based on the complexity of scattering interactions, it represents a model that is much too simplified. The cubic polynomial equation did a much better job at modeling the spectra; however, it still posed a number of limitations for a complete systematic analysis of the samples. We will consider these limitations next.

There are several problems in using theoretical equation fitting for modeling the scattering and absorbance properties of complex cosmoseutical formulations.

1. The Rayleigh scattering equation has too many variables to model properly.

2. The cubic polynomial fit can yield both negative and positive slopes depending on absorbance contribution.

3. The absorbance metric as well as the nanoparticle and large particle scattering component metrics are all on different scales so comparison impossible.

The solution to this problem was the development of an analytical method based on spectral areas under the curve which will be discussed in detail in the "Calculations" section.

Spectrophotometer Methodology

Samples can be characterized using a UV/Visible spectrophotometer equipped with a 150 mm Spectralon standard integrating sphere and center mount. Figure 2 is a picture of the Lambda 1050 UV/Vis/NIR instrument with the 150 mm sphere fitted into the detector compartment area of the instrument. Part of the reference and sample beam transfer optics can be seen on the left. The scatter transmission port can be seen in the center of the picture on the left hand side of the sphere. The diffuse reflectance port is under the blue cover on the right of the sphere. This sphere is fitted with a center mount accessory that can be seen on top and in the center of the sphere housing. The center mount will be a crucial component of this research.

Figure 2. 150 mm Integrating Sphere

What would be ideal would be a simple spectroscopic methodology that would allow for the characterization and quantitation of these three basic light interactions of absorbance, large particle scatter, and nanoparticle scatter. Samples that are solids, powders, or creams can be measured on a UV/Visible spectrophotometer equipped with a 150 mm standard integrating sphere. The optical diagram of a typical double beam integrating sphere can be seen in Figure 3a. The reference and sample beams are both measured by the sphere. For almost all measurements the reference bean strikes a Spectralon target.

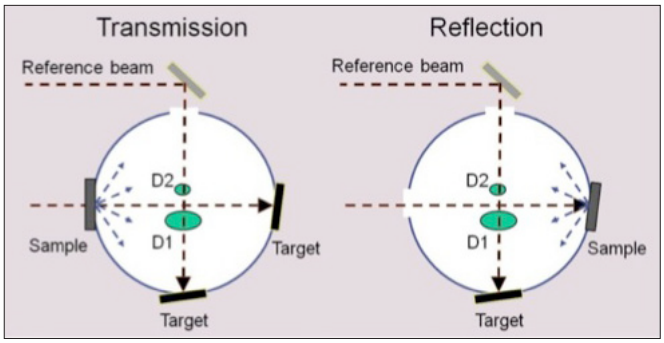

Figure 3a. Beam Path in a Typical Sphere

If the sample is placed in front of the sphere at the scatter transmission port, the transmitted and forward-scattered light is collected. This is depicted in Figure 3b at the bottom in blue. The diagram directly above it in red depicts the same sample placed on the opposite side of the sphere at the diffuse reflectance port. The diffusely reflected and back-scattered light is collected. Between these two different measurements, all of the scattered light from the sample is collected and measured. In scatter transmission and diffuse reflectance measurements, light can be lost to absorbance in a sample as well. This is demonstrated in the pink colored areas of the samples in both top and bottom parts of the figure.

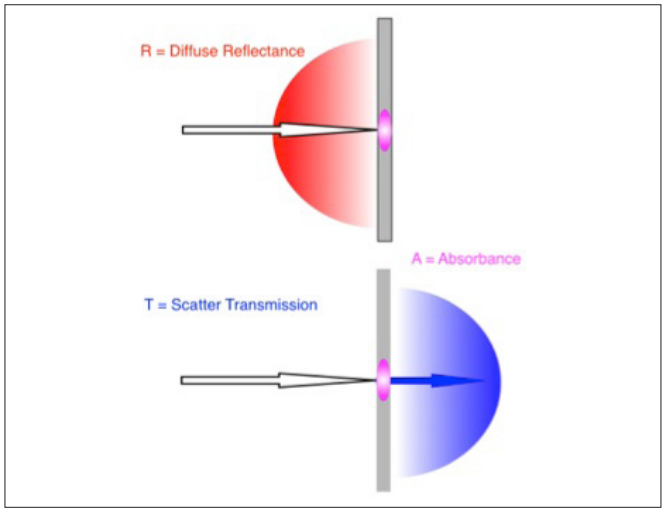

Figure 3b. Directionality of Scatter From a Flat Sample

All the samples evaluated by this method were either creams, semi-solid gels, or powders. Samples are first prepared for measurement; liquids are placed in a cuvette or gels and creams can be lightly spread on a frosted quartz plate. The samples are then measured on a UV/Visible instrument (PerkinElmer Lambdas 650\750\850\950\1050) equipped with a 150 mm integrating sphere with center mount. The instrument is background corrected with a Spectralon plate and the sample spectra are then measured in scatter transmission and center mount mode.

The samples were prepared for instrumental measurement in the following way. Lightly apply the material to the supportive substrate media (frosted quartz plate or Transpore Surgical Tape). The spectrophotometer is background corrected using a Spectralon reference plate, then measure %Transmission and %Reflectance spectrum by placing the sample containing substrate at the appropriate port on the sphere (see Figure 3a). For center mount measurements the spectrophotometer is background corrected with the Spectralon reference plate in place at the diffuse reflectance port and an empty center mount accessory in the sphere. The sample is then placed into the center mount, turned to a 10 degree angle of incidence and the sample measured.

In Figure 4a a "clip type" center mount is shown, this accessory is designed to hold a variety of flat samples. The "paddle " assembly at the bottom of the sphere prevents sample scattered light from directly entering the detectors before at least one bounce within the sphere. To prevent spectral artifacts it is desirable for the light from the sample to reflect multiple times from the interior of the sphere.

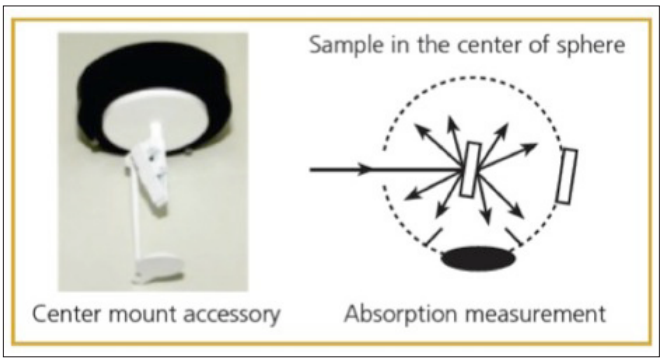

Figure 4a. The Center Mount and a Top View of a Center Mount Placed Sample

The diagram in Figure 4b displays how the center mount/sphere configuration collects all of the sample-scattered radiation through a full 360 degrees. A center mount sampling background, or a baseline measurement, is obtained with a sample in the center mount, however, the center mount is turned so that the beam does not illuminate it. In the diagram on the right, the sample measurement configuration is depicted with the sample oriented such that the instrument beam makes an 10 degree angle of incidence with the sample. This can also be seen on the right hand side of Figure 4a.

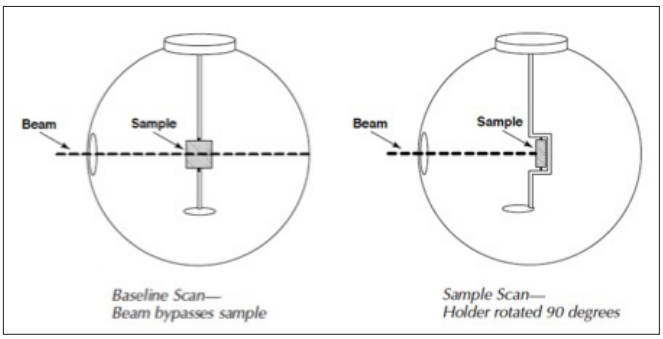

Figure 4B. Center Mount Fitted in a 150 mm Sphere

So does the center mount really collect all the scattered light? We can verify this by adding together the scatter transmission and diffuse reflectance spectra and then compare them to the center mount spectrum. If both the forward and backscatter are completely collected in the scatter transmission (solid green line) and diffuse reflectance (solid purple line) spectra respectively, they should add up to the center mount spectrum. In this graph are displayed spectra from a two ply layer of surgical tape, an artificial substrate used to mimic the spectral properties of human skin. The addition product of the reflectance and transmission spectra is the red dotted line spectrum. It overlays and compares with the center mount spectrum in solid black.

Figure 5 displays the transmission, reflection, and center mount spectra for a Transpore Surgical Tape sample. It is exemplary of typical data for this assay. With it we can verify that the center mount does indeed collect all of the scattered light. We do this by adding together the scatter transmission and diffuse reflectance spectra. Then, they are compared to the center mount spectrum. If both the forward and back scattered light are completely collected in the scatter transmission (solid green line) and diffuse reflectance (solid purple line) spectra respectively, they should add up to the center mount spectrum. This graph displays spectra from a two ply layer of surgical tape, an artificial substrate used to mimic the spectral properties of human skin. The red dotted line represents the addition product of the reflectance and transmission spectra. This line overlays and compares with the center mount spectrum in solid black transmission spectra. This line overlays and compares with the center mount spectrum in solid black.

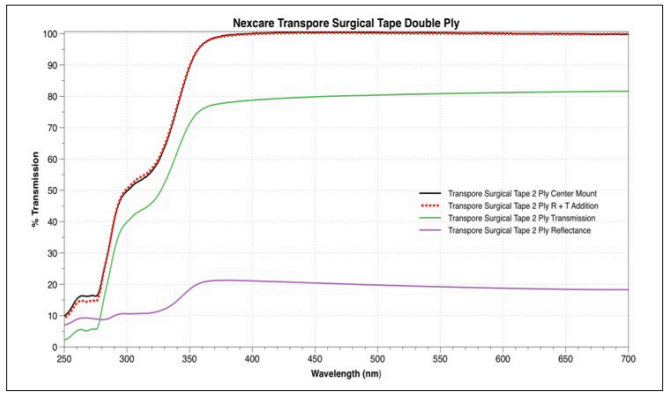

Figure 5. How Scattered Light Adds Up in Typical Sphere Measurements

Calculations

Figure 6 shows the spectral plan of attack for the problem. The visible region from 700 nm to 400 nm, in green highlight, will be used to analyze scattering and absorbance phenomena. The red highlighted UVA and UVB regions from 400 nm to 250 nm are the "business end" of the spectrum for sunscreens and SPF rated cosmetics. The ultra violet region is far more problematic to isolate nano and large particle scatter due to the significant absorbance of the carrier medium; however, SPF measurements can be calculated from both scatter transmission and center mount spectra. The top, black spectrum is from the center mount; whereas, the bottom grey spectrum is the scatter transmission measurement.

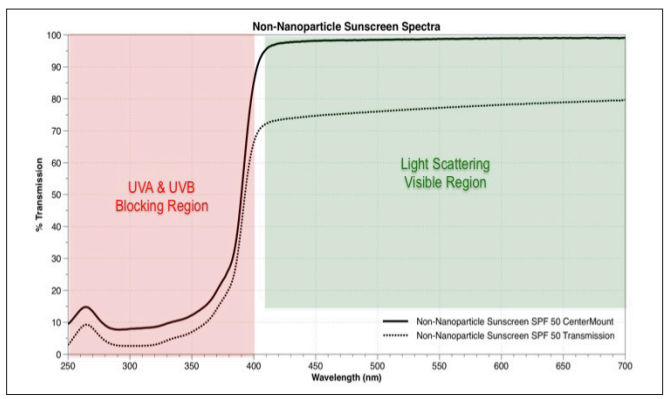

Figure 6. Analysis Regions in Measuring Scattering in Cosmetics and Sunscreens

The integrating sphere center mount accessory is the key instrumental feature that is critical to this analysis. Here are the three relevant points of the analysis.

1. In the center mount spectrum any values less than 100 %T are due exclusively to sample absorbance only.

2. Large particle scattering, from particles greater than approximately 800 nm, cause a wavelength independent % transmission offset in the center mount spectrum.

3. Small particle scattering, from particles lesser than approximately 800 nm, cause a wavelength dependent curving that increases with decreasing wavelength in the scatter transmission spectrum.

The comparison of a scatter transmission and center mount spectra gives one the ability to differentiate scatter from sample absorbance. This is a crucial step in isolating absorbance from scatter phenomena in this method. Without this ability pigmented cosmetics with a visible region absorbance would be impossible to characterize properly. Let take a look at a difficult absorbing/ scattering sample.

The pig skin sample shown in Figure 7 constitutes the topmost epidermal skin layer and is made up primarily of protein. As such, it has both an absorbing and scattering natural material mimicking the spectroscopy of human skin. The spectra are dominated by the large protein absorbance at 280 nm. There is also a pronounced curvature starting at 600 nm. But is the curvature due to nanoparticle scatter or a long wavelength absorbance decline?

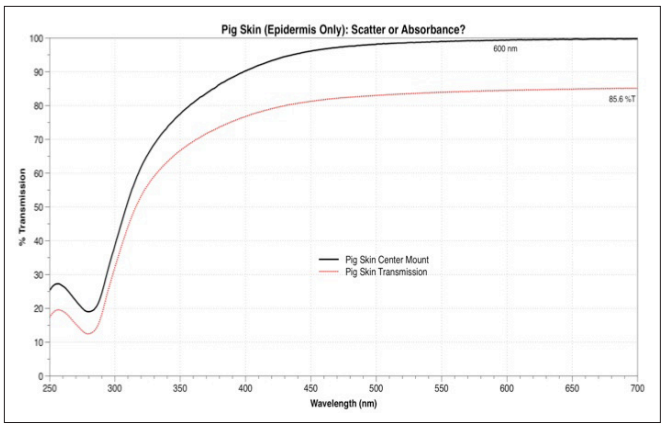

Figure 7. Scatter or Absorbance: Porcine Epidermis Sample

The center mount spectrum (black) indicates the absorbance contribution, isolated from any scattering component. In the scatter transmission spectrum (red) the offset at 700 nm from the center mount spectral value indicates a modest large particle scattering contribution. The conclusion from comparing the shape of the two spectra is that this sample has a significant absorbance along with a large particle scattering contribution with little or no nanoparticle scattering. This would be consistent with our knowledge of epidermal protein structures being polypeptide chains larger than the UV/Visible wavelengths. Clearly empirical visual inspection gives one a crude measure of the relative contribution of absorbance versus large and nanoparticle scattering, but clearly a better quantitation metric is needed.

The solution to a quantitative comparison of scatter and absorbance involves getting all three values on the same common scale. This can be accomplished with the use of spectral areas in combination with some simple algebra. Figure 8a shows the general layout. For the sake of simplicity we will consider spectra as sloping straight lines with the center mount spectrum in blue and the scatter transmission spectrum in brown. The shaded red visible region between 700 nm and 400 nm is our measurement area and has a maximal contribution from 100 %T to 0 %T of 30,000 spectral area units. All spectral areas are obtained from PerkinElmer's UVWinLab software.

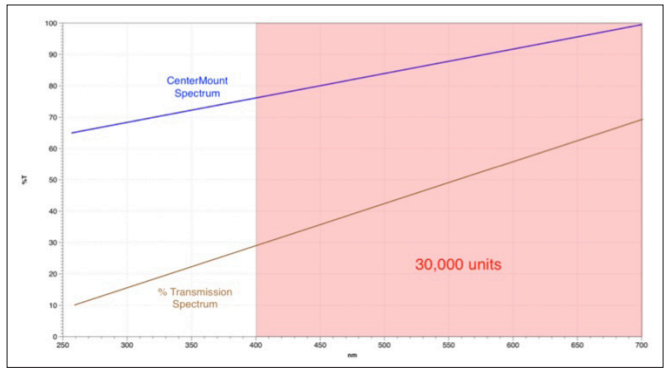

Figure 8a. Area Contribution of Visible Spectral Region

Sample absorbance, the shaded yellow region in Figure 8b, will always be the area between the center mount spectrum to a straight line at the of maximum 100 %T. This value can be calculated by subtracting the spectral area below the center mount spectrum, shaded blue, from the total visible region area of 30,000 units.

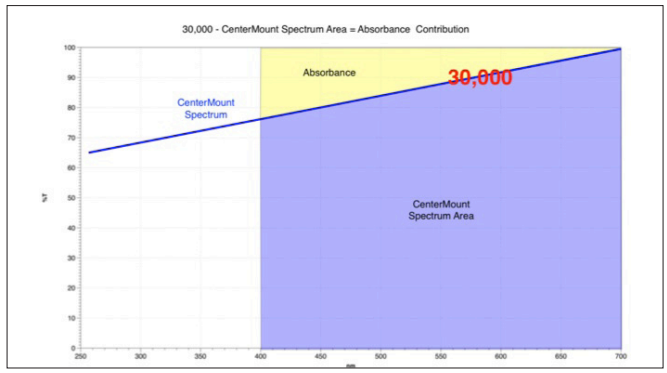

Figure 8b. Calculation of Absorbance Area Contribution

Calculation of the scattering components is a little more involved. The large particle contribution will be considered next. The first step is to calculate a %T extension area boundary line from the longest wavelength of the scatter transmission spectrum, represented by the dotted black line in Figure 8c. This line is representative of the wavelength independent %T offset due to large particle scattering; therefore, it maintains a constant value for all wavelengths in the UV and visible regions. To calculate the large particle contribution a subtraction of the %T extension area, shaded brown in Figure 8c, from the area beneath the center mount spectrum is performed. The result is the blue shaded area representative of large particle scatter.

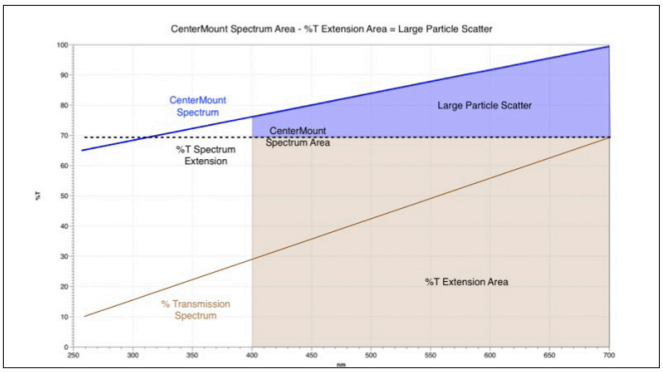

Figure 8c. Calculation of Large Particle Area Contribution

The nanoparticle scatter utilizes the %T extension line as well. Depicted in Figure 8d is the calculation of the nanoparticle scattering contribution. Again we use the %T extension area from the previous scatter calculation, dotted black line. From that value is subtracted the area below the %Transmission spectrum, shaded brown. The result is the red shaded nanoparticle area. What we are measuring is the curvature of the %Transmission spectrum that represent the wavelength dependent nanoparticle scatter.

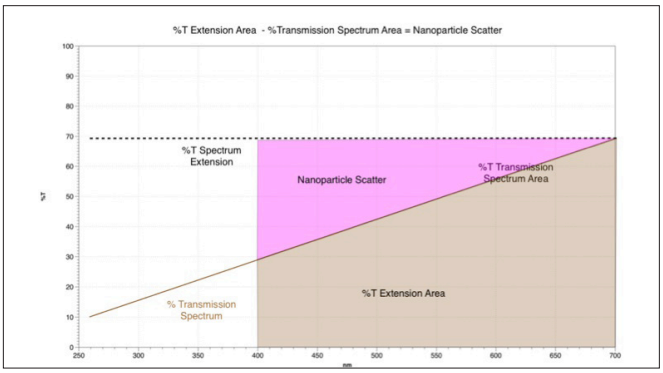

Figure 8d. Calculation of Small Particle Area Contribution

Displayed in Figure 8e is a combined representation of how all the spectral areas add up, along with their associated spectral and calculated boundaries. With this procedure it is possible to account for all of the scattering and absorbing phenomena occurring in a typical semi-transparent scattering sample. The absorbance is shown in yellow, the large particle scattering is in blue, and small particle (nanoparticle) scattering is in red.

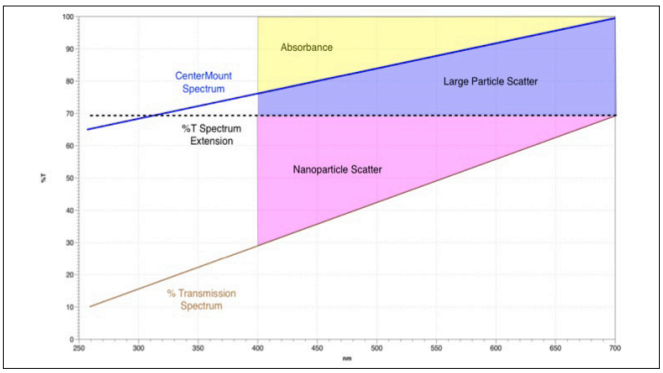

Figure 8e. All Calculated Areas For Absorbance and Scatter Components

There is one problematic configuration of the center mount with regard to the sample absorbance that can generate a bias in the calculation. This occurs when the sample has a significant absorbance that depresses the center ount spectrum below the %T extension value associated with large particle scatter within the visible spectral region shaded in gray. This situation is depicted in Figure 8f for the blue center mount spectrum at the point of the red arrow in the plot. The only solution is to compress the measurement area such that the intersection point, red arrow, is outside of the shortened analysis area. The more this area is compressed the greater the bias for the absorbance and large particle scatter values.

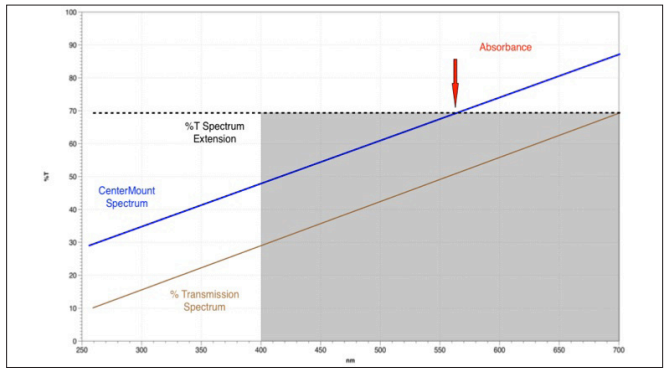

Figure 8f. One Problematic Configuration

In general, the spectral area procedure described here can be easily implemented in PerkinElmer's UVWinLab software as an automated turnkey calculation making the assay usable for quality control and formulation applications.

Data and Results

Let now turn our attention to data obtained with this method. First we will consider some common scattering artificial skin substrates used in calculating SPF values of sunscreens and cosmetics. This data will be important in demonstrating the quantitative potential for this methodology. Next we will move onto characterizing the full range of cosmetic products including ones that use organic blockers only, ones that use scattering particles only, and ones that use a mixture of both.

Artificial skin substrates are designed to mimic the absorbance and scattering properties of natural skin and are used as support media for SPF measurements. Considered here is Transpore Surgical Tape. Plotted in Figure 9 are the tape in one layer (black line) and two layers (red line). Note that both thickness have negligible absorbance above 370 nanometers as indicated by the solid red and black spectra for the center mount. All of the absorbance is in the UV region and is due to the polymer components of the tape. The dotted line spectra from the scatter transmission mode indicate that there is a significant scatter component which appears to correlate with tape thickness.

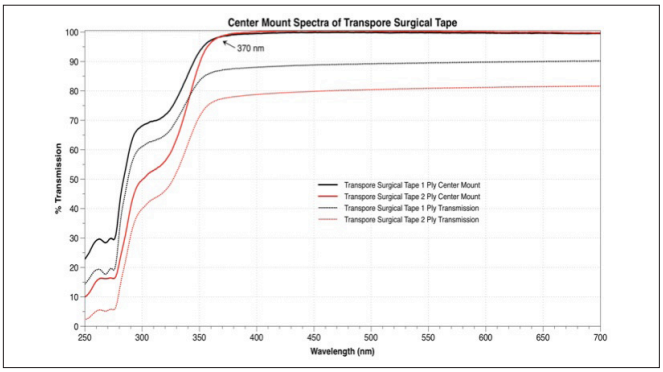

Figure 9. Typical Center Mount and % Transmission Spectra For Tape Substrates

Figure 10a compares data for a number of common artificial skin substrates. Each sample groups the values for absorbance (green), nanoparticle scatter (red), and large particle scatter (blue) areas. A comparison can then be made for a number of highly scattering materials. All samples appear to be significant large particle scattering materials with a much smaller nanoparticle scatter contribution. The absorbance is no more than noise level, with the exception of the pig skin discussed previously. The tapes and pig skin are all composed of polymeric molecules larger than the wavelength of incident light and the scatter data is consistent with these properties.

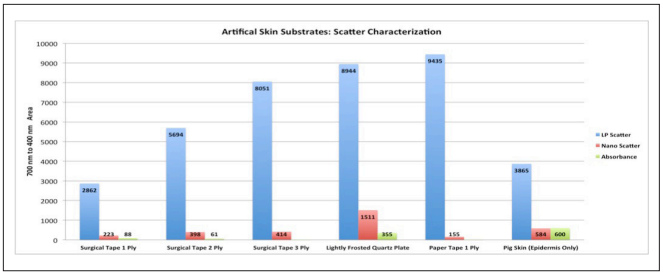

Figure 10a. Metrics of Various Scattering Materials

There is also a hint from the 1, 2, and 3 ply surgical tape samples plotted in Figures 10b and 10c that the scatter may be quantitated. Linear correlation least squares regression plots for large particle scatter (Figure10b) and nanoparticle scatter (Figure 10c) support this possibility. The large particle scatter has a better correlation (0.997) for sample thickness than the nanoparticle scatter data.

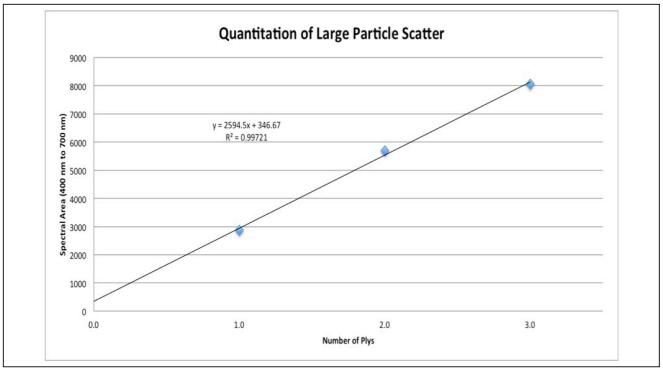

Figure 10b. Can Large Particle Scattering be Quantitated?

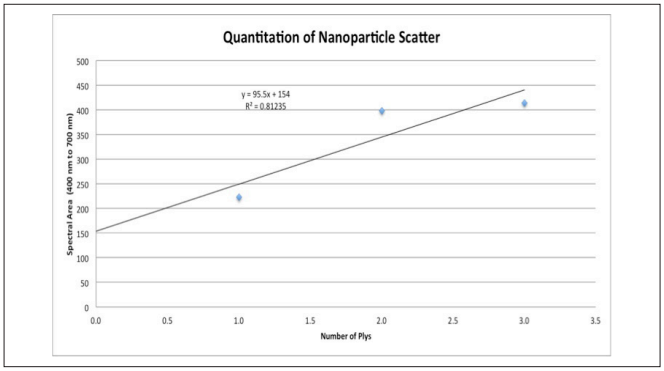

Figure 10c. Can Small (Nano) Particle Scattering be Quantitated?

To investigate the quantitative possibilities, a larger range of sample thickness needed to be investigated. As seen in the bar chart in Figure 11a, the tape is once again predominately a large particle scattering material. Linear least squares regression analysis for the scattering values verses sample thickness is show in Figures 11b and 11c.

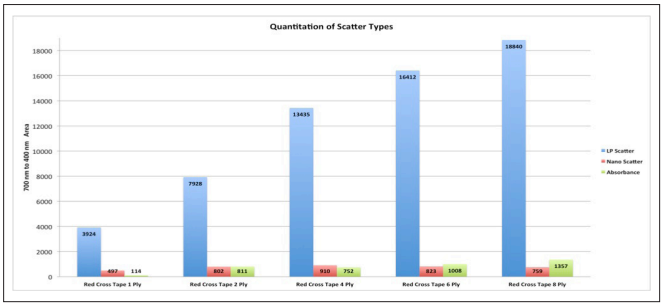

Figure 11a. Using Tape Layers to Validate Scatter Quantitation

A linear correlation (0.97) exists for large particle scatter through about a four ply thickness of tape or about two millimeters (Figure 11b). Nanoparticle scatter (Figure11c) is only linear for about a two ply thickness or approximately one millimeter. This is not unexpected since the thicker samples tend to have multiple scattering interactions that can diminish absolute scatter intensity. This phenomena is more pronounced for nanoparticle scatter; therefore, resulting in a smaller linear range and pronounce decrease with increasing thickness.

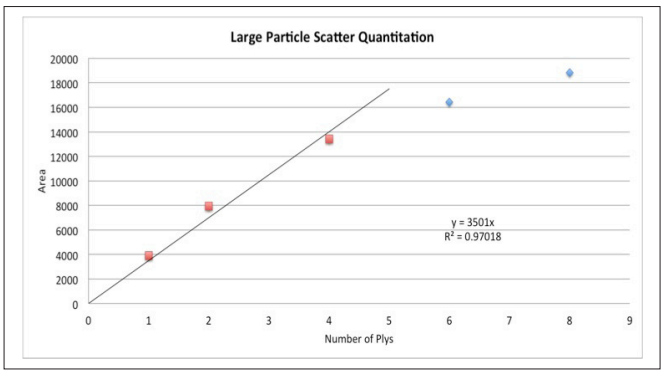

Figure 11b. Linearity for Large Particle Scatter Quantitation

Of relevance for the method is the fact that the thickness of the sunscreen and cosmetic samples will be only about 0.4 millimeters at maximum sampling thickness; thereby, well within the linear range for both types of scatter.

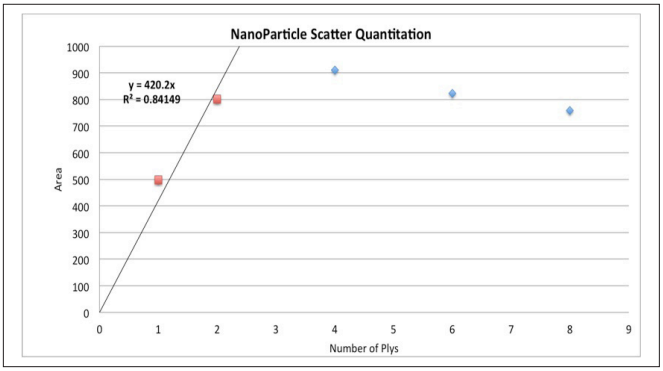

Figure 11c. Linearity for Small (Nano) Particle Scatter Quantitation

The theory behind UV protection inherent in sunscreens and cosmetics that have active ingredients of particulate zinc oxide and titanium dioxide is 1) small particles are very efficient at scattering shorter light wavelengths and 2) perceived reduced long term exposure toxicity of inert particles over benzenoid organic compounds. In order to gauge the contribution of nanoparticles in sunscreen and cosmetic formulations, we need to first get a baseline from sunscreens that have only absorbing, non-scattering, compounds as active ingredients.

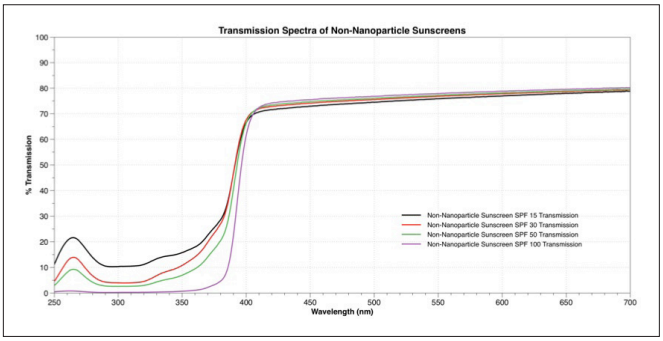

Figure 12a. Percent Transmission Spectra for Nanoparticle Free Sunscreens

Presented in Figure 12 are four sunscreens with progressively higher values of SPF factors ranging from 15 to 100. These sunscreens contain only organic UV blocking compounds, nanoparticles are not present as active ingredients. The scatter transmission spectra shown in Figure 12a and the center mount spectra in Figure 12b. The scatter transmission spectra have approximately a 20 %T offset from the maximum 100 %T; whereas, the center mount spectra spectra have a minimal offset and display little evidence of curvature between 700 nm and 400 nm.

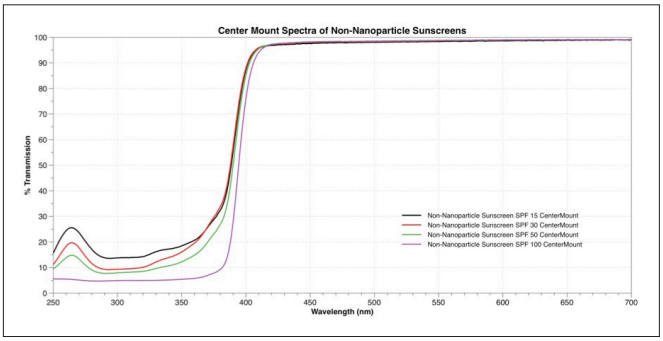

Figure 12b. Center Mount Spectra for Nanoparticle Free Sunscreens

Figure 13 shows a bar chart for the same four sunscreens comparing the spectral areas for absorbance (green), nanoparticle scatter (red), and large particle scatter (blue). These sunscreens have a significant contribution of large particle scattering associated with them. The scatter percentages appear to be somewhat uniform across the SPF range as well. The carrier medium for all of these sunscreens is an emulsion based cream which accounts for the dominant large particle scattering contribution. As expected there is only a slight absorbance contribution. For esthetic reasons, most sunscreens are designed to be transparent to visible radiation (400 nm to 780 nm).

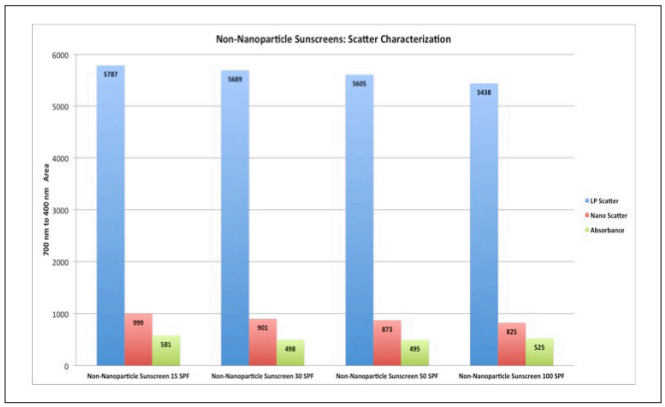

Figure 13. Metrics of Nanoparticle Free Sunscreens

There is one interesting aspect to the nanoparticle scattering value of the frosted quartz plate (see Figure 10a) used as a sample support substrate in comparison to the same plate with the sunscreens on applied. All the plate/ sunscreen values for nanoparticle scatter are lower than corresponding values for the empty plate. This is because the nanostructures associated with the surface of the frosted quartz plate are "filled in" by the components of the sunscreen carrier media, thereby, reducing the number of nano-scattering loci of the sunscreen/plate sample.

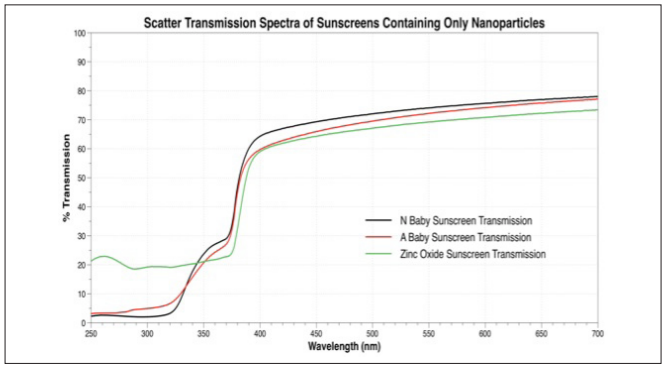

Figure 14a. Percent Transmission Spectra for Nanoparticle Containing Sunscreens

Considered next are sunscreens and cosmetics that contain only titanium dioxide or zinc oxide particles as active ingredients. Displayed in Figures 14a and b are spectra for three sunscreens that contain only nanoparticles as the active UV blocking ingredients. The scatter transmission spectra are in Figure 14a and the center mount spectra are in Figure 14b. From the center mount spectra we can see that these three sunscreens have little to no absorption, which is as expected, but there does appear to be more nanoparticle scatter based on the curvature of the scatter transmission spectra.

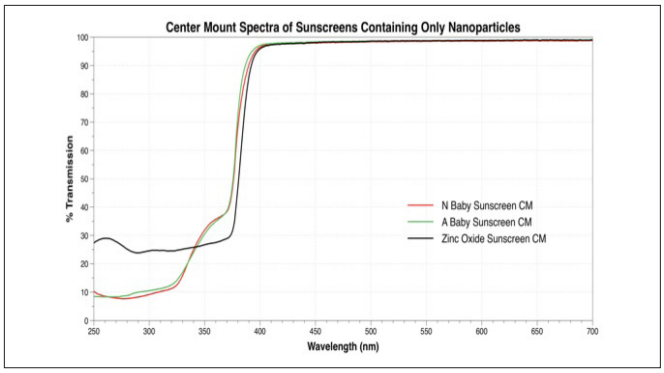

Figure 14b. Center Mount Spectra for Nanoparticle Containing Sunscreens

Plotted in Figures 14c and d are spectra for three cosmetic foundation products that contain only particles as the active UV blocking ingredients. The scatter transmission spectra are in 14c and the center mount spectra are in 14d. The biggest difference with cosmetic formulations is that they tend to be significantly pigmented to match and compliment the natural skin colors of the wearer. For cosmetic products the visible wavelength range absorbance can be substantial, especially product designed for darker skin tones. This can be seen in the structure of the spectra in the visible region of the center mount spectra. One cosmetic, the SB Foundation cream, is pigmented in the visible to the point that the assay range needed to be modified to 550 nm to 700 nm.

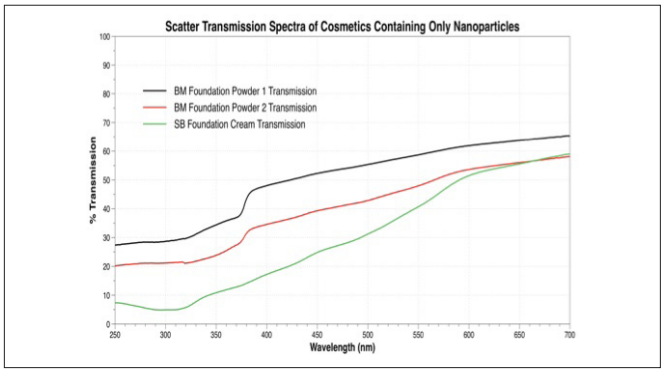

Figure 14c. Percent Transmission Spectra for Nanoparticle Containing Cosmetics

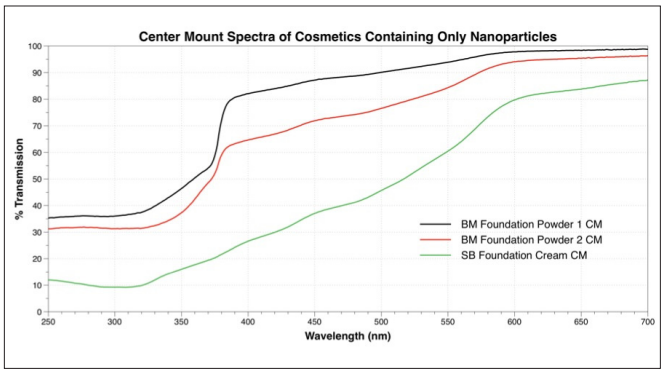

Figure 14d. Center Mount Spectra for Nanoparticle Containing Cosmetics

In Figure 15 spectral area data for this series of three sunscreens and three UV protective cosmetics is shown for evaluation and comparison. Again, both groups are composed of exclusively particle active ingredients. The three sunscreens are on the left, whereas the three cosmetics are on the right. The large particle scattering is about 25% higher for the nanoparticle products over the previous organic chemical only sunscreens. In addition, nanoparticle scattering is up by about 45% for the nanoparticle sunscreens verses the organic actives only counterparts, a clearly measurable contribution by the nanoparticles.

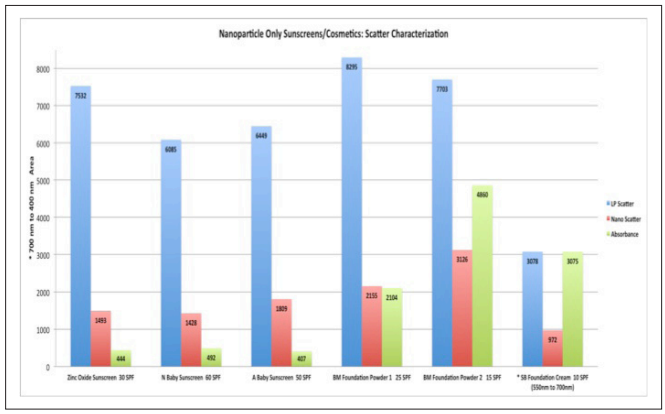

Figure 15. Metrics of Nanoparticle Containing Sunscreens and Cosmetics

The nanoparticle scatter contribution for the cosmetic samples showed an even larger increase of about 65% over their organic actives only sunscreen counterparts. Large particle scattering was increased as well for the cosmetics. The absorbance increase of the three cosmetics samples on the right of the chart is easily seen.

Why does the large particle scatter increase in these samples. The fact that both nanoparticle and large particle scatter increases with these materials may indicate a contribution from larger particles in the particulate raw ingredient used in formulation. Preliminary data from studies where the sunscreen is dissolved in an appropriate solvent indicates a marked increase in nanoparticle scattering in conjunction with a decrease in large particle scattering. This would be consistent with an aggregation phenomenon facilitated by the emulsion carrier matrix of the products.

The reduced calculation range of the last sample on the right may very well give anomalous results that bias the real contribution of the absorbance and scattering components.

Table 1. Sunscreen and Cosmetic Sample Active Ingredient Amounts

Name	SPF	Zn O%	TiO_2%	Total% Active
Zinc Oxide Sunscreen	30	20.0	0.0	20
N Baby Sunscreen	60	4.7	4.9	9.6
A Baby Sunscreen	50	6.8	8.1	14.9
BM Foundation Powder 1	25	10.0	25.0	35
BM Foundation Powder 2	15	5.0	15.0	20
S8 Foundation Cream	10	0.0	4.8	4.8

So do the scatter quantitation correlate with either the percentage of active ingredients or the stated label SPF factor? Table 1 lists the various particle compositions for the various sunscreens/cosmetics and their associated SPF factors. A linear correlation for the total percentage of active ingredient particles verses the SPF factor had a correlation coefficient value of 0.1. Clearly there is little correlation found here.

An additional linear correlation between nanoparticle scatter values verses the SPF factor yielded a very modest correlation coefficient of 0.57. While this indicates a simple trend, the trend had a negative slope for an inverse relationship between the two values. So as the SPF value increases the scattering contribution decreases. This would seen counter intuitive and the result may be simply fortuitous.

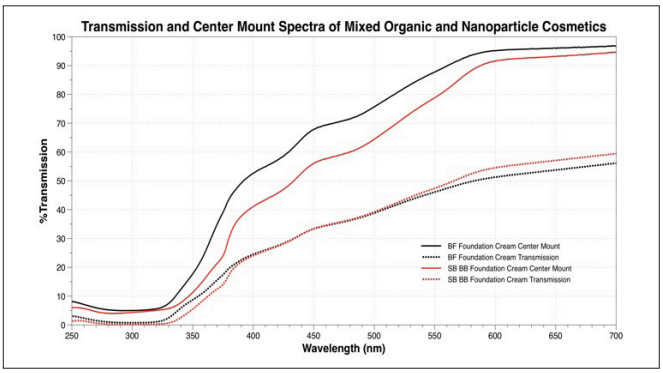

Figure 16. Spectra of Mixed Organic and Nanoparticle Cosmetics

Finally the most complex and difficult formulations. Cosmetics that include both organic chemical absorbers as well as scattering particles as active ingredients. These types of samples were selected to challenge the methodology with the most difficult formulation in terms of spectral complexity. To complicate the issue more these cosmetics are heavily pigmented.

The samples consist of two heavily pigmented foundation creams whose spectra are shown in Figure 16. The center mount spectra (solid lines) show clear evidence of significant absorbance from skin matching pigments. The absorbance effects go all the way into the long wavelength visible. In addition, there is clearly significant amounts of large particle scattering which can be noted in the scatter transmission spectra (dotted lines). At around 450 nm the absorbance is sufficient to cause problems with the area calculation. Both samples need to have the analysis range adjusted for the heavy absorbance.

The analysis range adjustments are fairly mild at 20 nm for the first sample and 70 nm for the second sample. Once the analysis range is shortened meaningful data can be obtained.

The area data is displayed in Figure 17. The elevated absorbance contribution for these types of pigmented cosmetics is clearly seen in the green bars. As in the previous particle containing cosmetics, the nanoparticle scatter values are significantly elevated over their organic chemical only counterparts.

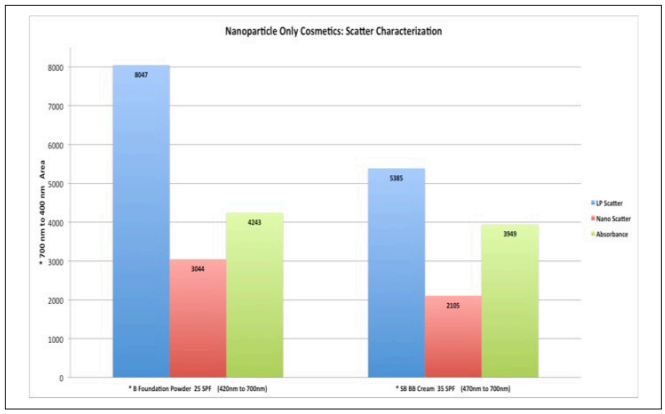

Figure 17. Metrics of Mixed Organic and Nanoparticle Cosmetics

Conclusion

Through the measurement and analysis of a wide range of commercially available sunscreen and cosmetic products, the methodology presented in this paper has allowed for the simultaneous quantitation and characterization of absorbance, large particle scattering, and nanoparticle scattering.

The methodology discussed in this paper has the advantage of being able to analyze a wide variety of physical types such as solids, liquids, suspensions, gels, creams, and films. More importantly it can characterize particles in their sample context, a particularly desirable capability for investigating phenomena such as aggregation.

In summary, the data indicated that compared to simple chemical only formulations 1) large particle scattering was from 7 % to 33 % higher in the nanoparticle containing formulations and 2) nanoparticle scattering was between 37 % and 72 % higher in nanoparticle containing formulations.

PerkinElmer, Inc.
940 Winter Street
Waltham, MA 02451 USA
P: (800) 762-4000 or
(+1) 203-925-4602
www.perkinelmer.com

PerkinElmer®

011362_01